Available online at www.sciencedirect.com
SCIENCE DIRECT®
Minerals Engineering 16 (2003) 1061–1068
MINERALS ENGINEERING
This article is also available online at:
www.elsevier.com/locate/mineng

Level control strategies for flotation cells

P. Kämpjärvi, S.-L. Jämsä-Jounela *

Laboratory of Process Control and Automation, Helsinki University of Technology, Kemistintie 1, 02150 Espoo, Finland

Received 23 April 2003; accepted 2 June 2003

Abstract

Flotation is a difficult process to run efficiently. One way to make flotation performance better is to improve cell level control. However, controlling pulp levels in flotation cells is a complex control task because of strong interactions between the levels in flotation cells. Therefore advanced controllers are needed to give good level control. This paper deals with a model of six flotation cells in series. Simulations are performed to compare different control strategies. Four control strategies are considered: one SISO controller and three different MIMO controllers including a new multivariable controller. It is shown that level control performances of the MIMO controllers are significantly better than that of the classical SISO controller.

Keywords: Flotation machines; Froth flotation; Process control; Mineral processing

1. Introduction

Level control of flotation cells is a very complex task due to high interactions between the process variables. A control action implemented at any point in the flotation circuit tends to be transmitted to both upstream and downstream units, and sometimes with amplification. Large variations in the flow rate to the first cell and varying composition of the raw ore also cause problems.

Flotation cells are conventionally controlled by isolated PI-controllers. PI control works well when the cell being controlled is isolated. However, in a flotation circuit where interactions are strong, PI control does not meet the requirements of high control performance. Hence a considerable amount of research has been carried out over the last few years to develop better control techniques for flotation circuits (Jämsä-Jounela et al., 2001).

Niemi et al. (1974), Koivo and Cojocariu (1977) used a single cell model when developing an optimal control algorithm via applications of the maximum principle. Andersen et al. (1979) and Zargiza and Herbst (1987) reported an application of state feedback control and a Kalman filter for rougher flotation control. Hammoude and Smith (1981) used a linear model to develop a minimum-variance controller for recleaning. New advanced control method has been also recommended for the control of flotation processes by (Stenlund and Medvedev, 2000).

The aim of this research is to study and compare different control strategies from the point of view of cell level control. In addition, a new control strategy is presented and implemented. Its performance is compared to three different strategies: one traditional SISO control strategy, and two MIMO control strategies. The strategies are compared by the means of special performance indices.

In the following the mathematical model of a flotation cell is first developed and a five cells in series cell configuration is constructed. The simulations are then performed in order to determine suitable control parameters for controllers of the cell levels. Simulation was performed with Matlab 5.2.0 and its Simulink library.

2. Mathematical modeling of flotation cells in series

In the flotation process the pulp is fed into the first cell and the froth is collected in the launders. The feed can be measured by a flow measurement, and the remaining pulp flows into the next cell. The magnitude of the flow depends on the pressure difference between two adjacent cells, the position of control valves, and the viscosity and density of the pulp. The magnitude of the pressure difference can be determined from the physical

* Corresponding author.
E-mail address: sirkka-l@hut.fi (S.-L. Jämsä-Jounela).

0892-6875/$ - see front matter
doi:10.1016/j.mineng.2003.06.004

height difference of the cells. The pulp level in a cell is measured and controlled by adjusting the control valve.

In the following a flotation cell is considered as a tank of perfectly mixed pulp. Since the pulp is perfectly mixed, the density is the same throughout the cell, i.e. there are no spatial density gradients in the cell. As the froth flow is small compared with the pulp flow, it is ignored in the outgoing flows. The impact of the air feed on the pulp level is also ignored.

The cells under study do not have the properties of ideal tanks because the cross-sectional area of the cell is not constant. A mathematical model for the physical properties will be developed and discussed next.

2.1. Single cells in series

In a flotation process several single cells are connected in series as shown in Fig. 1.

For the first cell in the series:

$$\frac{\partial V_1}{\partial t} = (q - F_1) = q - KC_v(u_1)\sqrt{y_1 - y_2 + h_1} \tag{1}$$

where q = feed rate to the first cell, y_1 = pulp level in the first cell, y_2 = pulp level in the second cell, h_n = physical difference in height between the cells, u_1 = control signal, K = constant coefficient, F_1 = outflow from the first cell, and C_v = valve coefficient.

The equations for cells 2, 3, and 4 are respectively (i = 2, 3, and 4)

$$\frac{\partial V_i}{\partial t} = (F_{i-1} - F_i) = KC_v(u_{i-1})\sqrt{y_{i-1} - y_i + h_{i-1}} - KC_v(u_i)\sqrt{y_i - y_{i+1} + h_i} \tag{2}$$

The equation for the last cell ($n = 5$)

$$\frac{\partial V_n}{\partial t} = (F_{n-1} - F_n) = KC_v(u_{n-1})\sqrt{y_{n-1} - y_n + h_{n-1}} - KC_v(u_n)\sqrt{y_n + h_n} \tag{3}$$

In the case of an ideal tank, the cross-section of a cell is assumed to be constant. The pulp levels in the cells can therefore be written as

$$\frac{\partial y_1}{\partial t} = \frac{(q - F_1)}{A_1} = \frac{q - KC_v(u_1)\sqrt{y_1 - y_2 + h_1}}{A_1} \tag{4}$$

$$\frac{\partial y_i}{\partial t} = \frac{K_{i-1}C_v(u_{i-1})\sqrt{y_{i-1} - y_i + h_{i-1}}}{A_i} - \frac{KC_v(u_i)\sqrt{y_i - y_{i+1} + h_i}}{A_i} \tag{5}$$

where i = 2, 3, and 4.

$$\frac{\partial y_n}{\partial t} = \frac{KC_v(u_{n-1})\sqrt{y_{n-1} - y_n + h_{n-1}}}{A_n} - \frac{KC_v(u_n)\sqrt{y_n + h_n}}{A_n} \tag{6}$$

where $n = 5$.

2.2. Double cells in series

Mathematical models for the double cells can be derived in a similar manner (Jämsä-Jounela et al., 2003). The principle differences compared with the mathematic models of single cells in series are that, in a double cell, both pulp levels are controlled by manipulating a control valve in the second cell outflow, as can be seen from Fig. 2. The cells are physically on the same level.

The pulp level in the second cell is measured and compared with the set point. This signal is used as input to a PI-controller. The output signal of the controller is the desired valve position as denoted by u_1. The cells in a double cell are connected via a flange. The flange limits the maximum flow between the cells. The pressure difference in the cells is the only driving force for the flow, and depends on the density of the pulp.

The velocity of outflow from the first cell can be derived using Bernoull's equation, resulting in

$$v = \sqrt{2g(y_1 - y_2)} \tag{7}$$

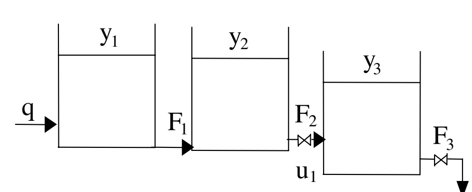

Fig. 2. Double flotation cell series.

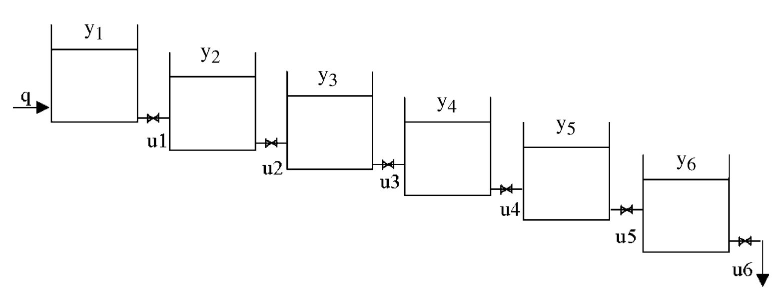

Fig. 1. Schematic diagram of flotation cells.

where g = gravity, y_1 = pulp level in the first cell, and y_2 = pulp level in the second cell.

The volume flow across the flange can be calculated as

$$F_1 = vA_{\text{flange}} = \sqrt{2g(y_1 - y_2)}l_1h_1 \tag{8}$$

where A_{flange} = cross-sectional area of the flange, l_1 = length of the flange, and h_1 = height of the flange.

The pressure drop due to flowing resistances is assumed to be negligible and can be ignored. The change of the pulp volume in the first cell with respect to time can be written as

$$\frac{\partial V_1}{\partial t} = q - F = q - \sqrt{2g(y_1 - y_2)}l_1h_1 \tag{9}$$

The outflow of the second double cell is similar to that of a single cell, and the flow into the second cell is the outflow of the first. Therefore the mathematical model is

$$\frac{\partial V_2}{\partial t} = F_1 - F = \sqrt{2g(y_1 - y_2)}l_1h_1 - K_2C_v(u_1)\sqrt{y_2 - y_3 + h_1} \tag{10}$$

2.3. Modelling the Outokumpu flotation cells

Fig. 3 shows the cross-section of the flotation cells under study. The pulp level changes as a function of the cell volume. The change is linear from the bottom of the cell to the starting level of the launders and boosters, denoted by $H_{\text{lowerpart}}$ in Fig. 3. The cross-section of the pulp subsequently decreases on moving upwards because the launders and 'boosters' reduce the volume of the cell.

Calculation of the pulp volume can be divided into two sections: the pulp level below and above the level of $H_{\text{lowerpart}}$. When the volume is smaller than the volume of the cylinder's $H_{\text{lowerpart}}$, the pulp level is determined as

$$h_{\text{tot}} = \frac{V}{\pi R_{\text{tot}}^2} \tag{11}$$

where R_{tot} is the radius of the cell.

If the pulp volume is equal or greater than $H_{\text{lowerpart}}$, the volume is written as

$$V = V_{\text{lowerpart}} + V_{\text{upperpart}}(h) - V_{\text{B}}(h) - V_{\text{R}}(h) \tag{12}$$

where $V_{\text{lowerpart}}$ = volume of the cell below the level of $H_{\text{lowerpart}}$, $V_{\text{lowerpart}}$ = volume of the cylinder above $H_{\text{lowerpart}}$, V_{B} = volume of the boosters, and V_{R} = volume of the launders.

A level variable, the zero point of which is equal to $H_{\text{lowerpart}}$ is denoted by h. The volumes of the launder and booster are obtained by geometric relations, and substituting them in Eq. 12 results in

$$h^3\left(-\frac{\pi}{3}K_{\text{B}}^2\right) + h^2(\pi K_{\text{B}}R_{\text{total}}) + h(\pi(K_R - R_{\text{total}}^2)) + (V - V_{\text{lowerpart}}) = 0 \tag{13}$$

where K_{B} = constant coefficient of the booster dynamics and K_{R} = constant coefficient of the launder dynamics.

The third order equation has a solution in $[H_{\text{lowerpart}}H_{\text{total}}]$, where H_{total} is the total height of the cell. K_{B}, K_{R} and $V_{\text{lowerpart}}$ are constants and specific for each cell size. The total level of pulp can be determined by summarizing h and $H_{\text{lowerpart}}$.

The effect of pulp level non-linearity can be seen in Fig. 4, in which the pulp level is presented in ideal tank conditions as a function of the pulp volume. The cell type is TC-50, the maximum volume of which is 50 m^3.

2.4. Valve sizing and characteristic curve of the valves

Valve sizing is based on the C_v value, which is calculated according to the ISA standard as follows:

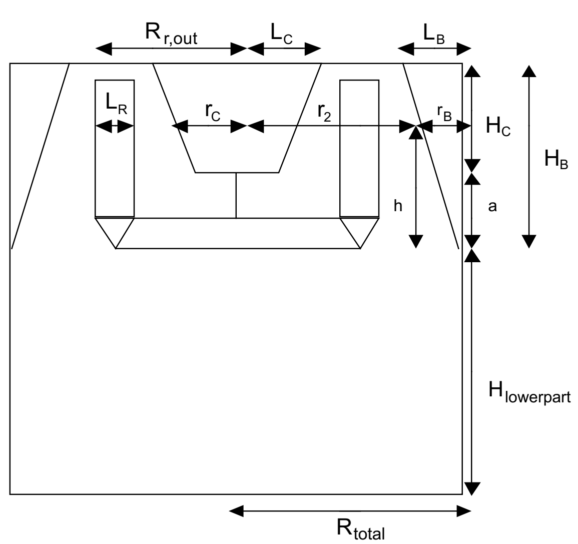

Fig. 3. Cross-section of a flotation cell of Outokumpu Mintec.

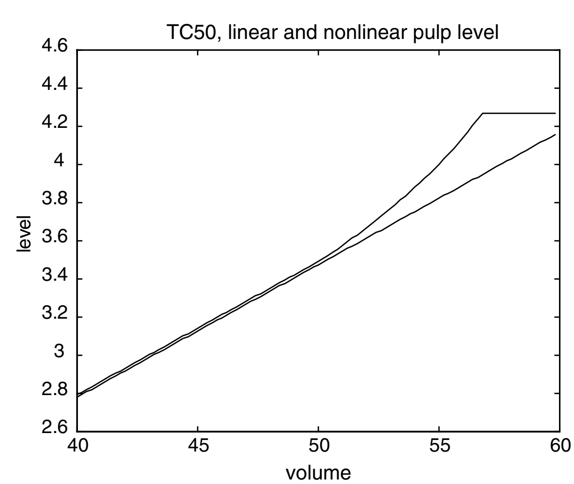

Fig. 4. Pulp level as a function of pulp volume.

$$C_v = 1.17Q \cdot \sqrt{\frac{\rho}{\Delta p}} \tag{14}$$

where Q is the flow rate (m^3/h), C_v the valve capacity coefficient, ρ the pulp density (kg/m^3), and Δp the pressure difference over the valve.

The flow rate (m^3/h) through the cell is calculated as

$$Q = 1.2\frac{V_{cell}}{\tau/60} \tag{15}$$

where V_{cell} is the cell volume (m^3) and τ the pulp retention time in the cell.

The valves in the models are sized for a flow which has a retention time of 1.5 min in one cell. The flow rate to the first cell is also calculated using this retention time value.

Characteristic curves of the control valves are produced by Larox Flowsys and were used in the Simulink models in order to cause realistic and non-linear behavior for the valves.

3. Control strategies

The different control strategies are discussed and described in the following sections. These strategies are selected because they can be used with basic PI-controllers and without any additional instrumentation. Traditionally in flotation cell series there is only one flow measurement in the beginning of the series and level PI-controllers in every cell.

3.1. Feed-forward controller

A flow feed-forward controller monitors disturbances in the inflow to the first cell and uses proportional action to close or open the valves of the cell in order to compensate for disturbances. Compensation is linearly dependent on the difference between the current inflow and the normal inflow. The measurement signal is filtered in order to prevent the feed-forward control from reacting to random variation in the flow. However, this kind of controller does not provide any extra performance improvement in the event of disturbances occurring somewhere else in the cell series. The model of the feed-forward controller is shown in Fig. 5.

3.2. Decoupling controller

A decoupling controller is based on differential equations (1)–(3). The purpose of the decoupling controller is to eliminate the crosswise effects of control loops, and hence the stability of a single control circuit depends only on its own stability features. The basic model of the decoupling controller is shown in Fig. 6.

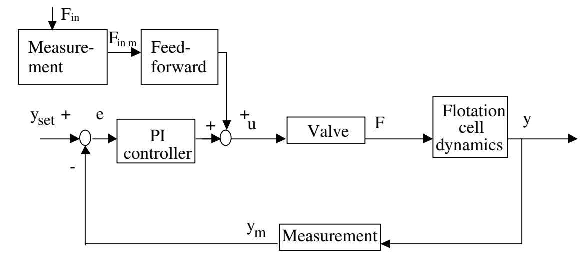

Fig. 5. Control diagram of feed-forward controller.

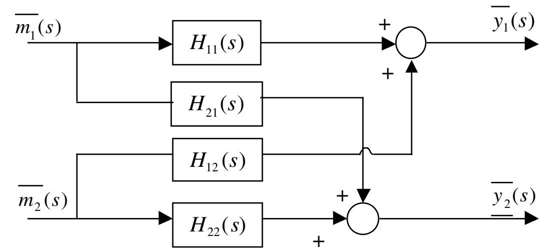

Fig. 6. Control diagram of a basic decoupling controller.

The mathematical criterion to be fulfilled for decoupling a tank i will be

$$\Delta F_{i\,\mathrm{in}} - \Delta F_{i\,\mathrm{out}} = 0 \tag{16}$$

where $\Delta F_{i\,\mathrm{in}}$ is a change of inflow to tank i. Using the valve functions from Eqs. (1)–(3) the equation can be written as follows

$$F_i = K_i C_{vi} u_i \sqrt{(\Delta h_i)} \tag{17}$$

where Δh_i is the level difference over the valve. Substituting in Eq. (16), it becomes

$$\begin{aligned} &K_{i-1}C_{i-1}(u_{i-1} + \Delta u_{i-1})\sqrt{(\Delta h_{i-1} + \Delta(\Delta h_{i-1}))} \\ &\quad - K_i C_i(u_i + \Delta u_i)\sqrt{(\Delta h_i + \Delta(\Delta h_i))} = 0 \end{aligned} \tag{18}$$

Solving this equation for the change in the control signal gives

$$\begin{aligned} \Delta u_i &= (K_{i-1}C_{i-1}/K_iC_i)u'_{i-1}\sqrt{(\Delta h'_{i-1})/(\Delta h'_i)} - u_i \\ &= f\left(u'_{i-1}, \Delta h'_{i-1}, \Delta h'_i\right) \end{aligned} \tag{19}$$

Eventually, the control signal for a tank i becomes

$$u_i = u_{PI} + f(u_{i-1}, \Delta h_{i-1}, \Delta h_i) \tag{20}$$

where u_{PI} is the control signal from a PI-controller. In order to handle the variations from the inflow, the feed-forward is attached to the first tank.

3.3. Multivariable controller similar to Floatstar™

A multivariable controller (Schubert et al., 1995) controls the total inventory of material in the upstream tanks. In this control strategy, controlling a valve is influenced not only by the difference between a set point and the measured level in the tank, but also the differences between set points and the measured levels in all the tanks in upstream. These variables are summed and fed to the PI-controller of the cell. Furthermore, the variables are scaled by a suitable factor depending on the valve size, position and process.

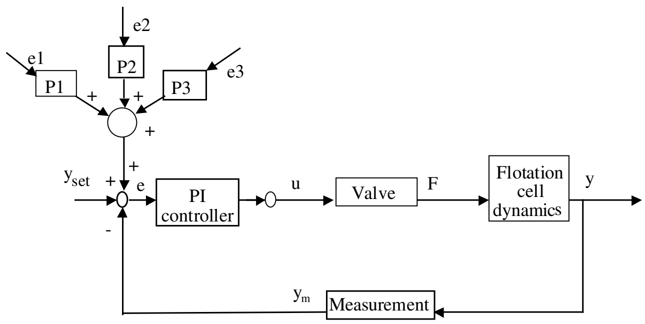

Fig. 7. Control diagram of a multivariable controller similar to Floatstar™ (tank 4).

In this strategy each control valve can be regarded as a sluice gate of a dam. When a damned inventory is too high in upstream, the valves are opened more than usual, even when there seems to be no need to take such an action on the basis of the levels in the neighboring vessels. The control diagram is shown in Fig. 7.

3.4. New multivariable controller

When some disturbance occurs in tank, it has an effect to level in the previous tank in upstream. Previously

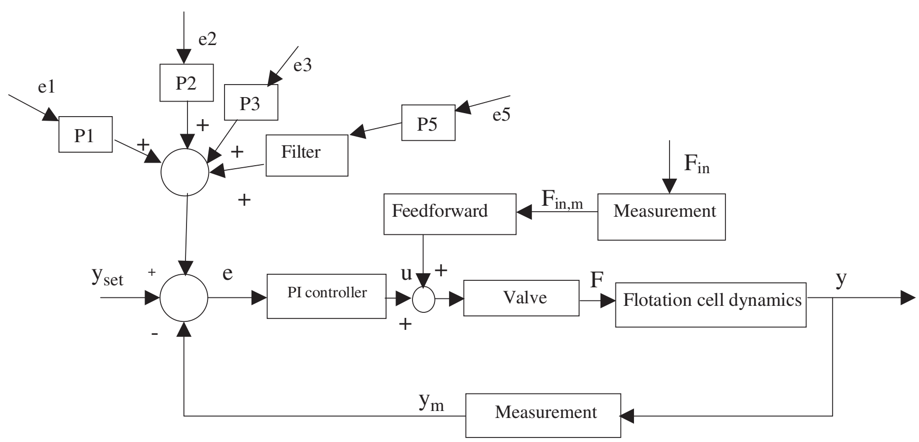

Fig. 8. The control diagram of MV controller (tank 4).

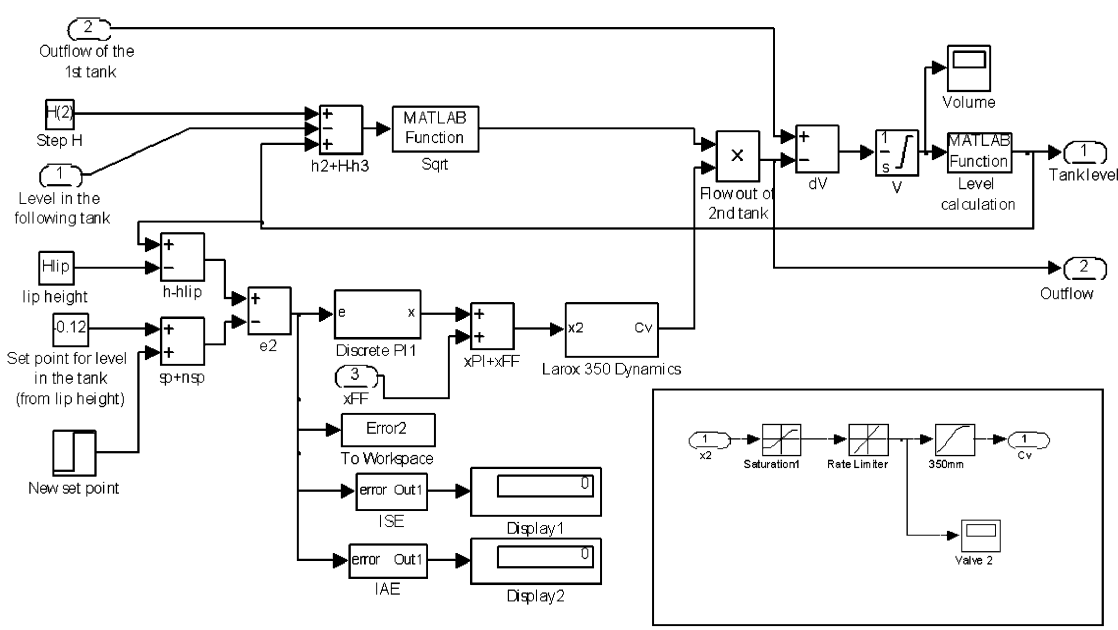

Fig. 9. Simulink model of the flow dynamics in a flotation cell.

described multivariable control does not take disturbances of this kind into account. Also strategy does not take into account disturbances arising from pulp feed. Therefore a flow feed-forward has been added to the system and the difference between set point and measured level in next tank is also added to the controller of previous tank. The control diagram is shown in Fig. 8.

4. Simulations

In the simulations a configuration of six TC-50 cells in series was studied in accordance with the ideal tank assumption. Therefore the effects of boosters and launders were not considered. The valves were 100% oversized according to the ISA standard, and the retention time in each cell was 1.5 min. Control strategies included conventional PI-controllers with feed-forward control, decoupling controller, a multivariable controller similar to Floatstar$^{\mathrm{TM}}$ and a feed-forward multivariable controller. The simulation results of a +3 cm change in the set points of the cell levels at times 100, 150, 200, 250, 300 and 350 s are presented in the following. Making ±20% change in the feed to the first flotation cell was also simulated with different strategies. The set point of the cell level is lowest in the first cell, and the set point values increase on moving towards the last cell in the series, where the operating range of the level controller is smaller. The simulation schemes were constructed with Matlab 6.0.0 Simulink software. The Simulink model of the flow dynamics in the flotation cell is presented in Fig. 9.

The controllers were tuned and compared using the following indices. The IAE index (integral of the absolute value of the error) integrates the absolute value of errors, and even-handedly weights all the deviations. ISE (integral of the square error) gives more weight to big deviations from the set point.

$$\mathrm{ISE} = \int_{t=t_1}^{t_2} (y(t) - y_{\mathrm{sp}}(t))^2 \,\mathrm{d}t \tag{21}$$

$$\mathrm{IAE} = \int_{t=t_1}^{t_2} |y(t) - y_{\mathrm{sp}}(t)| \,\mathrm{d}t \tag{22}$$

5. Simulation results

The simulations of the configurations of six TC-50 cells in series resulted in parameters for the PI-controllers. Integration times in the traditional system with a feed-forward controller were between 15 and 50 s and proportional gains between 0.8 and 1.2. Because MIMO control strategies respond better to disturbances, the PI parameters were set faster. Integration times in all the PI-controllers were set to 15 s and gain to 1. In the de-

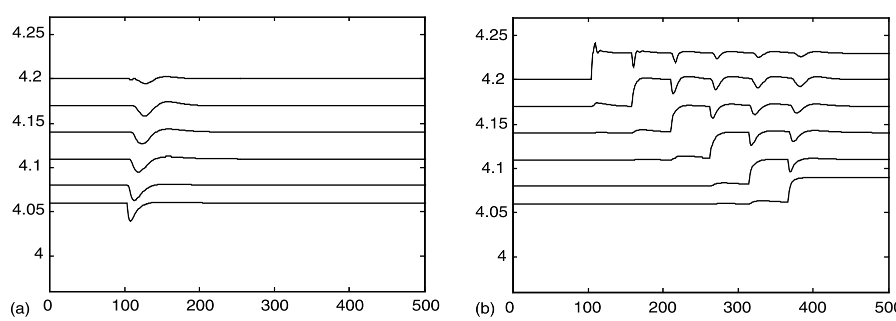

Fig. 10. Feed-forward controller. On the left the response to a −20% change in pulp feed, and on the right the response to set point changes.

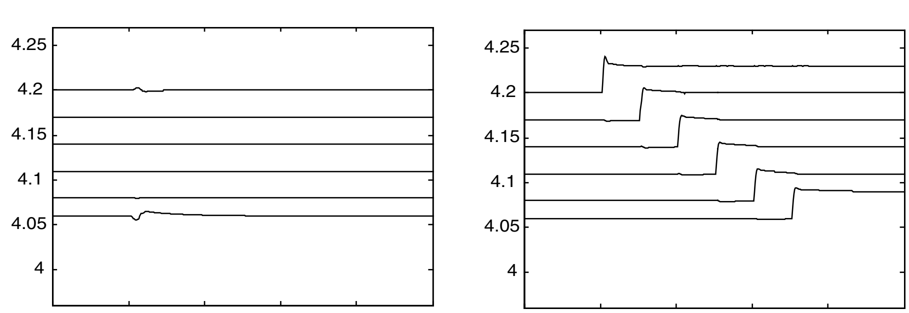

Fig. 11. Decoupling controller. On the left the response to a −20% change in pulp feed, and on the right the response to set point changes.

coupling controller the PI-parameters were between 15–50 s and 1–1.4 s, correspondingly.

The responses of the feed-forward controller to disturbances in pulp feed and to set point changes are presented in Fig. 10. As can be seen, the −20% change in pulp feed is affecting all the cell levels in the series. The set point changes in a cell also have undesirable effects on the adjacent cells. There is always a considerably large perturbation in the level of the next cell every time a set point change is made in the system.

The responses of the decoupling controller are illustrated in Fig. 11. The decoupling controller is a MIMO controller, and it also takes into account the interactions between cells. As can been seen from the graphs, the decoupling controller effectively eliminates disturbances arising from changes in the pulp feed. Furthermore, set point changes in the cells do not affect to the other cells.

The responses of configurations in which a controller similar to Floatstar™ and the new multivariable controller are used are shown in Figs. 12 and 13. The new multivariable controller seems to be more robust than the other controller, especially during changes in pulp feed.

The IAE and ISE indices, which depict the performance of controllers, are shown in Tables 1–4. As was to be expected, the traditional SISO control with flow feed-forward had the poorest figures in all cases.

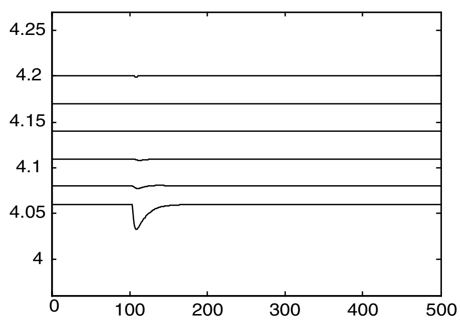

Fig. 12. Multivariable controller similar to Floatstar™. On the left the response to a −20% change in pulp feed, and on the right the response to set point changes.

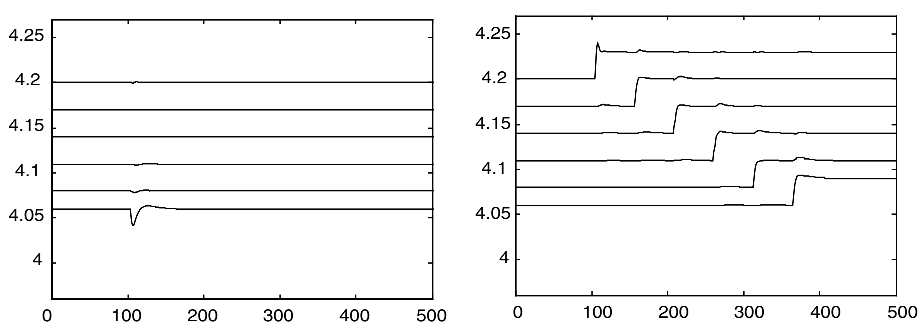

Fig. 13. New multivariable controller. On the left the response to a −20% change in pulp feed, and on the right the response to set point changes.

Table 1
The performance indices for the feed-forward controller

Feed-forward controller	ISE(+20%)	IAE(+20%)	ISE(−20%)	IAE(−20%)	ISE(s.p.c.)	IAE(s.p.c.)
1	3.1	348	3.7	325	2.7	298
2	2.9	361	3.1	360	4.0	520
3	2.7	371	3.3	391	5.0	712
4	2.2	341	2.7	371	5.33	818
5	2.0	322	2.4	361	6.5	970
6	0.5	159	0.4	147	3.7	604

Table 2
The performance indices for the decoupling controller

Decoupling controller	ISE(+20%)	IAE(+20%)	ISE(−20%)	IAE(−20%)	ISE(s.p.c.)	IAE(s.p.c.)
1	1.1	327	0.7	263	2.0	220
2	0.0008	10.2	0.0003	8.0	2.2	242
3	0.0000008	0.3	0.00000004	0.1	2.2	241
4	0.00000005	0.05	0.000000001	0.01	2.2	241
5	0.00003	1.2	0.000004	0.4	2.1	228
6	0.04	29.5	0.019	19.5	2.1	179

Table 3
The performance indices for the multivariable controller similar to Floatstar™

MV controller	ISE(+20%)	IAE(+20%)	ISE(−20%)	IAE(−20%)	ISE(s.p.c.)	IAE(s.p.c.)
1	7.81	499	9.02	527	2.2	202
2	0.1	65.0	0.07	58.6	2.3	243
3	0.03	25.2	0.03	26.5	2.3	248
4	0.0001	2.2	0.00006	1.4	2.3	249
5	0.0001	2.7	0.00008	1.5	2.3	245
6	0.01	18.5	0.002	7.8	1.7	151

Table 4
The performance indices for the new multivariable controller

New MV controller	ISE(+20%)	IAE(+20%)	ISE(−20%)	IAE(−20%)	ISE(s.p.c.)	IAE(s.p.c.)
1	1.79	216	2.1	231	2.2	204
2	0.03	30.7	0.02	27.4	2.2	202
3	0.007	12.3	0.007	13.2	2.2	211
4	0.0001	1.1	0.00009	1.7	2.2	211
5	0.0009	4.3	0.0005	3.5	2.2	212
6	0.005	8.1	0.003	6.9	1.9	149

6. Conclusions

All the simulated configurations were successfully tuned. It is noticeable that the classical SISO strategy with feed-forward controller cannot even approach the performances of the MIMO controllers. This is due to high interactions between the control loops, which SISO systems cannot take into account.

The differences between different MIMO systems are somewhat smaller. All the controllers performed robustly to disturbances in pulp feed and to set point changes. The decoupling controller had the best IAE and IDE indices. However, the decoupling controller is sensitive to model uncertainties (Skogestad and Postelwaite, 1996). This also means that process changes can strongly degrade the control performance.

References

Andersen, R., Gronli, B., Olsen, T., Kaggernd, I., Ramslo, K., Sandvik, K., 1979. An optimal control system of the rougher flotation at the Folldal Verk concentrator, Norway. In: Proceedings of the 13th International Mineral Processing Congress. New York, USA, pp. 1517–1540.

Hammoude, A., Smith, H., 1981. Experiments with self-tuning control of flotation. In: Proceedings of the 3rd IFAC Symposium on Automation in Mining, Mineral and Metal Processing. Oxford, UK, pp. 213–218.

Jämsä-Jounela, S.-L., Laurila, H., Karesvuori, J., Timperi, J., 2001. Evaluation of the future automation trends in control and fault diagnostics—a case study in flotation plant. In: 10th IFAC Symposium on Automation in Mining, Mineral and Metal Processing.

Jämsä-Jounela, S.-L., Dietrich, M., Halmevaara, K., Tiili, O., 2003. Control of pulp levels in flotation cells. Control Engineering Practise, 73–81.

Koivo, H., Cojocariu, R., 1977. An optimal control for a flotation circuit. Automatica 13 (1), 37–45.

Niemi, A., Maijanen, J., Nihtilä, M., 1974. Singular optimal feed forward control of flotation. In: IFAC/IFORS Symposium on Optimization Methods—Applied Aspects. Varna, Bulgaria, pp. 277–283.

Schubert, J.H., Henning, R.G.D., Hulbert, D., Craig, I.K., 1995. Flotation control—a multivariable stabilizer. In: XIXth IMPC, San Fransisco, vol. 3, pp. 237–241.

Skogestad, S., Postelwaite, I., 1996. Multivariable Feedback Control: Analysis and Design. John Wiley & Sons.

Stenlund, B., Medvedev, A., 2000. Level control of cascade coupled flotation tanks. Future trends in automation in mineral and metal processing. In: Jämsä-Jounela, S.-L., Vapaavuori, E. (Eds.), IFAC Workshop 2000, Helsinki, Finland, pp. 194–199.

Zargiza, R., Herbst, J.A., 1987. A model based feed forward control scheme for flotation plants. In: 116th AIME annual meeting. Denver, CO, USA, pp. 23–27.